Supporting Information

One-pot, One-step, Label-free miRNA Detection Method Based on the Structural Transition of Dumbbell Probe

Jae Hoon Jeung [a,b], *Hyogu Han* [a,c], *Se Hee Jang* [a,d] *Chang Yeol Lee* [e*], *Jun Ki Ahn* [a*]

[a] Material & Component Convergence R&D Department, Korea Institute of Industrial Technology (KITECH), Ansan, Republic of Korea

[b] Department of Biological Engineering, College of Engineering, Konkuk University, Seoul 05029, Republic of Korea

[c] Department of Chemistry, Gangneung-Wonju National University, Gangneung, 25457, Republic of Korea

[d] Department of Medical Device Engineering and Management, College of Medicine, Yonsei University, Seoul 03722, Republic of Korea

[e] Bionanotechnology Research Center, Korea Research Institute of Bioscience and Biotechnology (KRIBB), 125 Gwahak-ro, Yuseong-gu, Daejeon, 34141, Republic of Korea

*Corresponding author

Jun Ki Ahn, Ph.D.

Tel.: +82-31-8040-6391; E-mail address: jkahn@kitech.re.kr

Chang Yeol Lee, Ph.D.

Tel.: +82-42-860-4456; E-mail address: lcyeol8457a@kribb.re.kr

Table S1. Oligonucleotide sequences were used in this work.

Oligonucleotide sequence (5'□ 3')	
ODP 5*	Phos/GTACGACAACTACCCCATACCAAACCTTCCTTCGTACCCCTATAGTGAGTCG TATTATCATCTTTACCAGACAGTGTTACGACTCACTATAGGG
ODP 6*	Phos/GTACGACAACTACCCCATACCAAACCTTCCTTCGTACCCCTATAGTGAGTCG TATTATCATCTTTACCAGACAGTGTTAGACTCACTATAGGG
ODP 7*	Phos/GTACGACAACTACCCCATACCAAACCTTCCTTCGTACCCCTATAGTGAGTCG TATTATCATCTTTACCAGACAGTGTTAACTCACTATAGGG
ODP 8*	Phos/GTACGACAACTACCCCATACCAAACCTCCTTCGTACCCCTATAGTGAGTCGT ATTATCATCTTTACCAGACAGTGTTACTCACTATAGGG
IDP 5*	Phos/GTACGACAACTACCCCATACCAAACCTTCCTTCGTACTAATACGACTCACTA TCATCTTTACCAGACAGTGTTACCCTATAGTGAGTCGTATTA
IDP 6*	Phos/GTACGACAACTACCCCATACCAAACCTTCCTTCGTACTAATACGACTCACTT CATCTTTACCAGACAGTGTTACCCTATAGTGAGTCGTATTA
IDP 7*	Phos/GTACGACAACTACCCCATACCAAACCTTCCTTCGTACTAATACGACTCACTC ATCTTTACCAGACAGTGTTACCCTATAGTGAGTCGTATTA
IDP 8*	Phos/GTACGACACTACCCCATACCAAACCTTCCTTCGTACTAATACGACTCATCAT CTTTACCAGACAGTGTTACCCTATAGTGAGTCGTATTA
AT probe	AGGAAGGTTTGGTATGGGGTAGTTG
20 bp T7p	TAATACGACTCACTATAGGG
15 bp T7p	TAATACGACTCACTA

*The colors orange, blue, and green represent the sequences of Mango aptamer, toehold, and miRNA 141 complementary, respectively.

Table S2. Oligonucleotide sequences were used in this work.

Oligonucleotide	sequence (5'□ 3')
miR-141	UAACACUGUCUGGUAAAGAUGG
miR-155	UUAAUGCUAAUCGUGAUAGGGGU
miR-21	UAGCUUAUCAGACUGAUGUUGA
miR-429	UAAUACUGUCUGGUAAAACCGU
miR-375	UUUGUUCGUUCGGCUCGCGUGA
miR-122	UGGAGUGUGACAAUGGUGUUUG
M1*	UAACACUGUCUGGUAAAGAUCG
M2*	UCACACUGUCUGGUAAAGAUCG
M3*	UCACACUGUCUGCUAAAGAUCG
M4*	UCAAACUGUCUGCUAAAGAUCG
M5*	UCAAACUGUCUGCUAAACAUCG

*The color reds represent the sequences of mismatches, respectively.

Table S3. Comparison with previously reported methods on miRNA detection.

Method	Time (min)	Reaction step	Limit detection	Maximum temperature (°C)	Ref.
RCA(CRISPR/Cas12a)	230	4	34.7 pM	95	[1]
RCT(CRISPR/Cas13a)	136	4	586 fM	80	[2]
HRCA(CRISPR/Cas13a)	163	5	200 aM	80	[3]
SDA + CHA	350	5	12 aM	95	[4]
SDA + Transcription	120	3	195 aM	95	[5]
TRCA	85	3	550 pM	65	[6]
DP-RCT	60	1	73 pM	34	This work

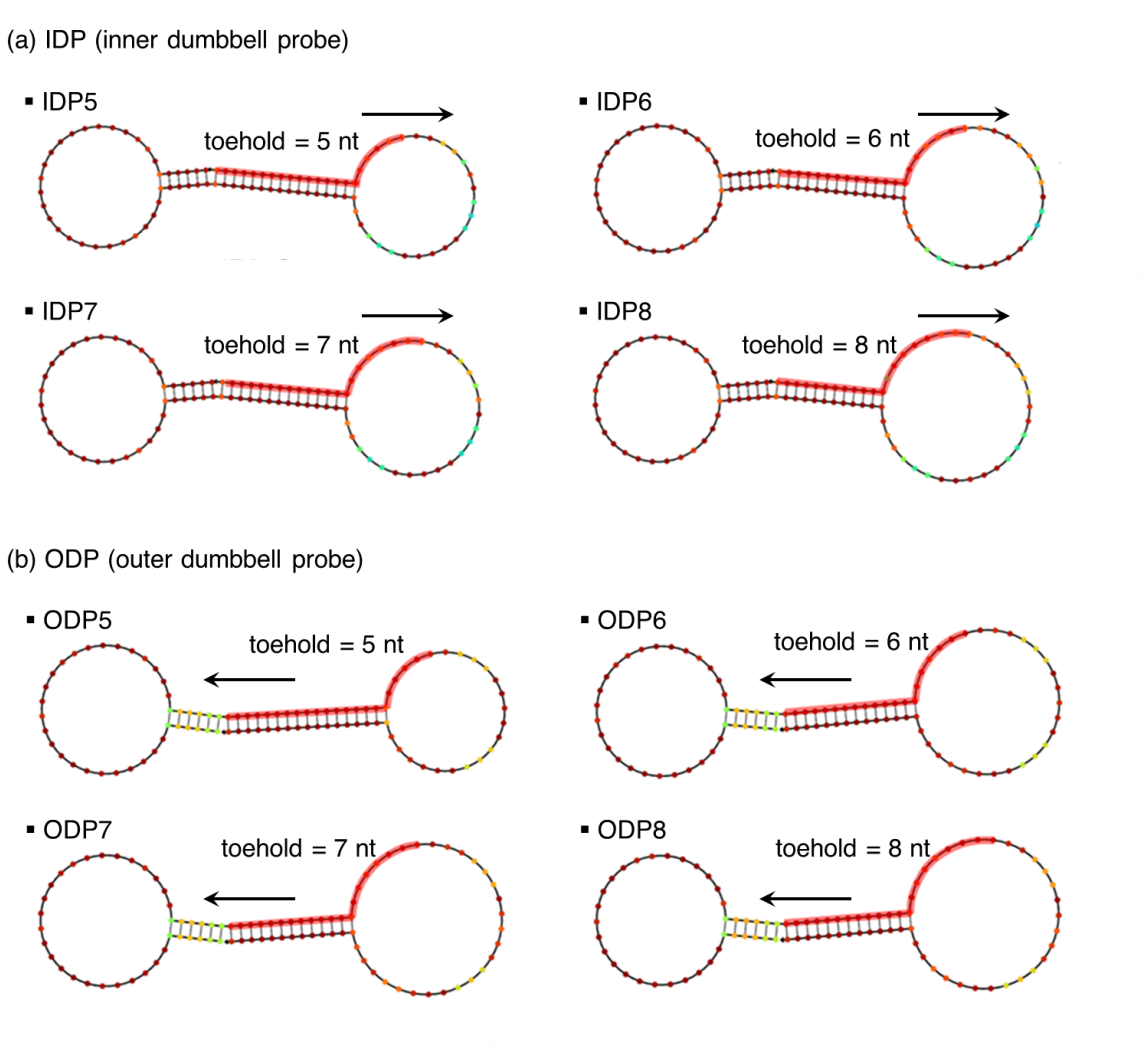

Figure S1. The nucleic acid structures of the various (a) IDPs and (b) ODPs created using the NUPACK nucleic acid modeling tool. The transparent red bold line and the black arrow indicates the sequences complementary to the T7 promoter and transcription direct (3' to 5'), respectively.

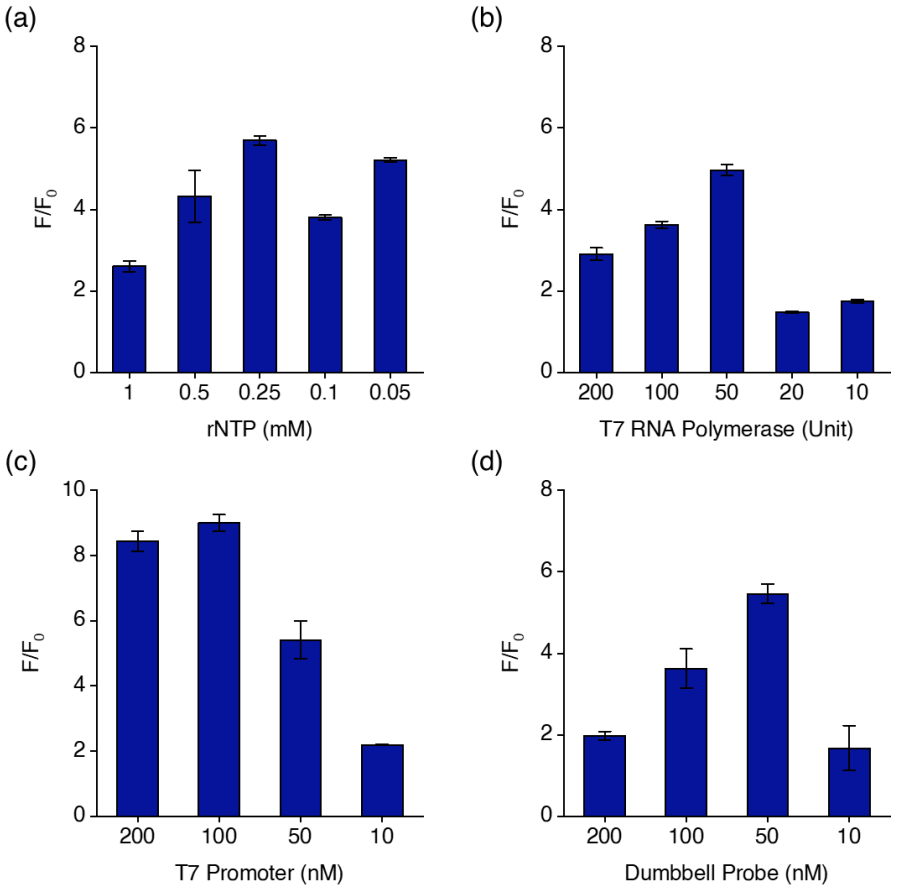

Figure S2. The optimization of the concentration of (a) rNTP, (b) T7 RNA polymerase, (c) T7p (T7 promoter), and (d) DP (dumbbell probe) for DP-RCT. The relative fluorescence intensity is defined as F/F_0, where F and F_0 indicate the fluorescence intensity from the samples with and without the target miR-141, respectively. The error bars indicate the standard deviations obtained from triplicate measurements.

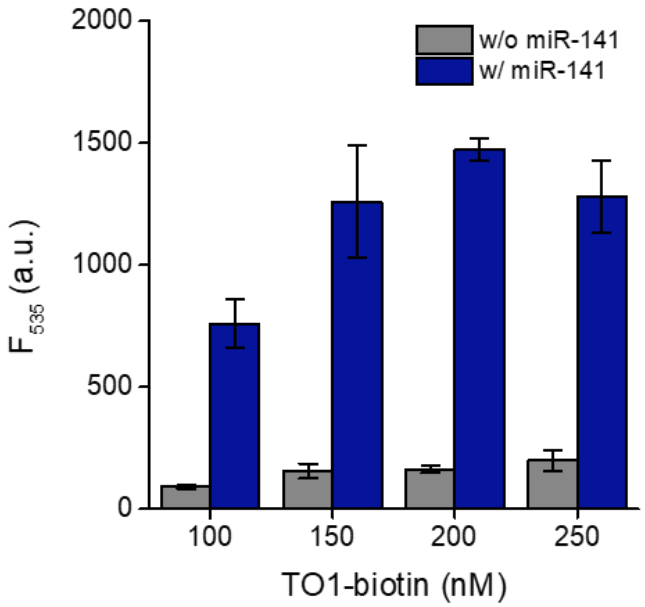

Figure S3. The optimization of concentration TO-1 biotin for DP-RCT. The relationship between the fluorescence intensity at 535 nm and the concentration of miR-141. The error bars indicate the standard deviations obtained from triplicate measurements.

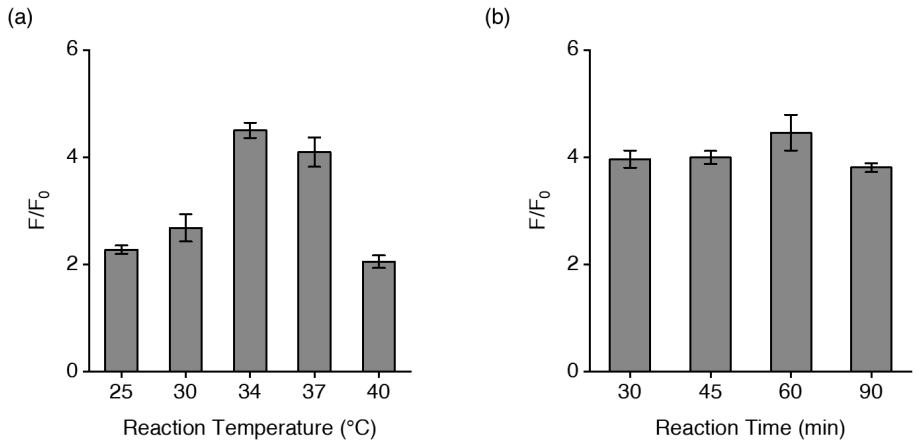

Figure S4. The optimization of reaction condition on (a) reaction time and (b) reaction temperature for DP-RCT. The relative fluorescence intensity is defined as F/F_0, where F and F_0 indicate the fluorescence intensity from the samples with and without the target miR-141, respectively. The error bars indicate the standard deviations obtained from triplicate measurements.

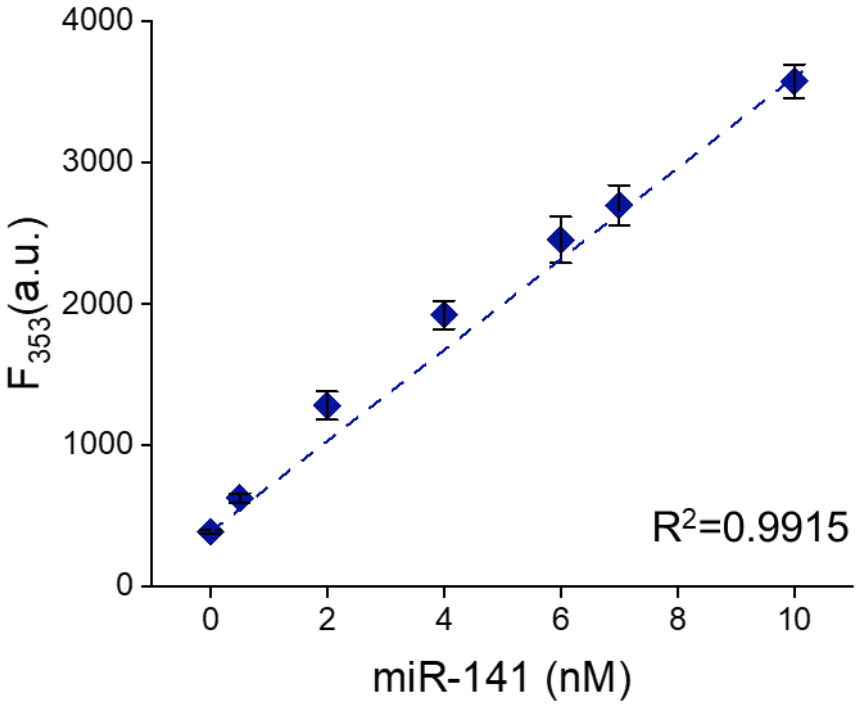

Figure S5. The fluorescence intensity as a function of miR-141 concentrations in 2% human serum. The relationship between the fluorescence intensity at 535 nm and the concentration of miR-141.

References

[1] G. Zhang, L. Zhang, J. Tong, X. Zhao, J. Ren, CRISPR-Cas12a enhanced rolling circle amplification method for ultrasensitive miRNA detection, Microchemical Journal. 158 (2020). https://doi.org/10.1016/j.microc.2020.105239.

[2] X. Ma, F. Zhou, D. Yang, Y. Chen, M. Li, P. Wang, miRNA Detection for Prostate Cancer Diagnosis by miRoll-Cas: miRNA Rolling Circle Transcription for CRISPR-Cas Assay, Anal Chem. (2023). https://doi.org/10.1021/acs.analchem.3c02231.

[3] M. Huang, R. Huang, H. Yue, Y. Shan, D. Xing, Ultrasensitive and high-specific microRNA detection using hyper-branching rolling circle amplified CRISPR/Cas13a biosensor, Sens Actuators B Chem. 325 (2020). https://doi.org/10.1016/j.snb.2020.128799.

[4] E. Xu, Y. Feng, H. Yang, P. Li, L. Kong, W. Wei, S. Liu, Ultrasensitive and specific multi-miRNA detection based on dual signal amplification, Sens Actuators B Chem. 337 (2021). https://doi.org/10.1016/j.snb.2021.129745.

[5] T. Yoon, S. Kim, J. Shin, Y. Zhou, K.S. Park, Highly sensitive multiplex detection of microRNA using light-up RNA aptamers, Sens Actuators B Chem. 330 (2021). https://doi.org/10.1016/j.snb.2020.129410.

[6] D. Kim, J. Lee, S. Park, J. Park, M.J. Seo, W.J. Rhee, E. Kim, Target-Responsive Template Structure Switching-Mediated Exponential Rolling Circle Amplification for the Direct and Sensitive Detection of MicroRNA, Biochip J. 16 (2022) 422–432. https://doi.org/10.1007/s13206-022-00071-2.